2-27-2015

Probing the Transition State Region in Catalytic CO Oxidation on Ru

H. Öström
Stockholm University

H. Öberg
Stockholm University

H. Xin
SLAC National Accelerator Laboratory

Jerry L. LaRue
Chapman University, larue@chapman.edu

M. Beye
SLAC National Accelerator Laboratory

See next page for additional authors

Recommended Citation

H. Öström, H. Öberg, H. Xin, J. LaRue, M. Beye, M. Dell'Angela, J. Gladh, M. L. Ng, J. A. Sellberg, S. Kaya, F. Sorgenfrei, G. Mercurio, D. Nordlund, W. F. Schlotter, A. Föhlisch, M. Wolf, W. Wurth, M. Persson, J. K. Nørskov, F. Abild-Pedersen, H. Ogasawara, L. G. M Pettersson, A. Nilsson, Probing the Transition State Region in Catalytic CO Oxidation on Ru, *Science* 2015, 347, 978-982, DOI: 10.1126/science.1261747

Probing the Transition State Region in Catalytic CO Oxidation on Ru

Authors
H. Öström, H. Öberg, H. Xin, Jerry L. LaRue, M. Beye, M. Dell'Angela, J. Gladh, M. L. Ng, J. A. Sellberg, S. Kaya, G. Mercurio, D. Nordlund, M. Hantschmann, F. Hieke, D. Kühn, W. F. Schlotter, G. L. Dakovski, J. J. Turner, M. P. Minitti, A. Mitra, S. P. Moeller, A. Föhlisch, M. Wolf, W. Wurth, M. Persson, J. K. Nørskov, F. Abild-Pedersen, H. Ogasawara, L. G. M. Pettersson, and A. Nilsson

Title: Probing the Transition State Region in Catalytic CO Oxidation on Ru

Authors: H. Öström[1], H. Öberg[1], H. Xin[2], J. LaRue[2,3], M. Beye[2,4], M. Dell'Angela[5], J. Gladh[1], M. L. Ng[2], J. A. Sellberg[1,2], S. Kaya[2], G. Mercurio[5], D. Nordlund[6], M. Hantschmann[4], F. Hieke[5], D. Kühn[4], W. F. Schlotter[7], G. L. Dakovski[7], J. J. Turner[7], M. P. Minitti[7], A. Mitra[7], S. P. Moeller[7],A. Föhlisch[4,8], M. Wolf[9], W. Wurth[5,10], M. Persson[11], J. K. Nørskov[2,3], F. Abild-Pedersen[3], H. Ogasawara[6], L. G. M Pettersson[1], A. Nilsson[1,2,6]*

Affiliations:

[1] Department of Physics, AlbaNova University Center, Stockholm University, SE-10691, Sweden

[2] SUNCAT Ctr Interface Sci & Catalysis, SLAC National Accelerator Laboratory, 2575 Sand Hill Road, Menlo Park, CA 94025, USA

[3] SUNCAT Ctr Interface Sci & Catalysis, Department of Chemical Engineering, Stanford University, Stanford, CA 95305, USA

[4] Helmholtz Zentrum Berlin für Materialien und Energie GmbH, Albert-Einstein-Strasse 15, D-12489 Berlin, Germany

[5] University of Hamburg and Center for Free Electron Laser Science, Luruper Chausse 149, D-22761 Hamburg, Germany

[6] Stanford Synchrotron Radiation Lightsource, SLAC National Accelerator Laboratory, 2575 Sand Hill Road, Menlo Park, CA 94025, USA

[7] Linac Coherent Light Source, SLAC National Accelerator Laboratory, 2575 Sand Hill Road, Menlo Park, CA 94025, USA

[8] Fakultät für Physik und Astronomie, Universität Potsdam, Karl-Liebknecht-Strasse 24-25, 14476 Potsdam, Germany

[9] Fritz-Haber Institute of the Max-Planck-Society, Faradayweg 4-6, D-14195 Berlin, Germany

[10] DESY Photon Science, Notkestr.85, D-22607 Hamburg, Germany

[11] Surface Science Research Centre and Department of Chemistry, The University of Liverpool, Liverpool, L69 3BX, UK

*Correspondence to: nilsson@slac.stanford.edu

Abstract:

Femtosecond x-ray laser pulses are used to probe the CO oxidation reaction on Ru initiated by an optical laser pulse. On a timescale of a few hundred femtoseconds, the optical laser pulse excites motions of CO and O on the surface allowing the reactants to collide and, with a transient close to a picosecond (ps), new electronic states appear in the O K-edge x-ray absorption spectrum. Density functional theory calculations indicate that these result from changes in the adsorption site and bond-formation between CO and O with a distribution of OC—O bond lengths close to the transition state (TS). After 1 ps 10 % of the CO populate the TS region, which is consistent with predictions based on a quantum oscillator model.

Main Text:

The transition state (TS) is the key to understanding chemical reactivity (*1*). It separates reactants from products and the free energy required to reach it determines the kinetics of an elementary chemical reaction. Molecules in the TS are hard to capture or observe because the short lifetime leads to a near-zero TS population at steady-state conditions. Ultrafast pump-probe techniques have, however, opened up opportunities for probing molecular structures near the TS region by promoting a sufficient population of molecules to allow detection on short time scales (*1, 2*). In particular, a number of dissociation and isomerization processes of single molecular units have

This material is based upon work supported by the U.S. Department of Energy, Office of Science, Office of Basic Energy Sciences, under Contract No. DE-AC02-76SF00515 and LDRD.

been probed with visible and infrared laser pulses (*1*). Much of chemistry, however, involves bimolecular reactions where new chemical bonds are formed. Previous pump-probe experiments have been performed in cases where reactants in the gas phase are brought together as a van der Waals complex or in liquid phase reactions between solute and solvent. These experiments could follow the bimolecular reaction dynamics and detect intermediates, but a direct spectroscopic probing of the TS region has proved a challenge (*3-5*). We take the next step and probe the TS region through time-resolved snapshots of the valence electronic structure in a surface-catalyzed bimolecular reaction.

A catalyst modifies the TS substantially, opening new reaction pathways that can lead to higher reactivity and selectivity (*6, 7*). Furthermore, the surface in heterogeneous catalysis and the metal center in homogeneous catalysis both facilitate the reaction by bonding the reacting molecular fragments in close proximity. This opens up the prospect of probing bimolecular reactions on ultrafast timescales where the reacting adsorbed species are present at neighboring sites and are brought to collide rapidly by optical excitation. Optical lasers can drive surface reactions on ultrafast timescale (*8-14*) and in particular the reaction between adsorbed CO and O to form CO_2 on metal surfaces which occurs within a few picoseconds (ps) (*11, 12,14*). The ability to probe species on surfaces on ultrafast time scales has recently taken a major leap forward with the development of free-electron x-ray lasers delivering ultrashort pulses combined with atom-specific spectroscopic tools to monitor the electronic structure (*15-17*). In a first exploitation of this technique, a short-lived intermediate precursor state was detected in CO desorption from Ru using x-ray emission spectroscopy (XES) and x-ray absorption spectroscopy (XAS) (*16*).

We demonstrate that ultrafast pump-probe x-ray spectroscopy based on the Linac Coherent Light Source (LCLS) x-ray free-electron laser (*18*) can be used to probe the electronic structure of molecular species in the TS region during CO oxidation on a Ru surface. With an optical laser pump pulse, we excited the electrons in the substrate. Subsequent energy transfer to the adsorbate system led to a rapid increase in adsorbate-substrate vibrational excitations, which then drove the CO oxidation reaction on ultrafast timescales. Using O K-edge XAS, we followed the time evolution of the unoccupied valence electronic structure around the adsorbed O and CO in an element-specific way during the oxidation process. Both the O and CO adsorbed species were activated within a few hundred femtoseconds upon laser excitation. This result suggests an ultrafast energy transfer to the adsorbed species from surface electrons excited by the laser pulse. After a delay on the order of 800 fs, new electronic states appeared, indicating the existence of new adsorbed species that do not resemble the separate systems in terms of CO molecules or O atoms adsorbed on the Ru surface. By comparing the experimental data to calculations of XA spectra these new resonances are identified as due to CO shifted from on-top towards hollow sites, O from hollow sites towards bridge sites and the formation of a bond between CO and O that is substantially elongated in comparison to the CO_2 final product. From the computed potential energy surface for the reaction, these fragments can be identified as molecular species being in the TS region while attempting to form CO_2. Based on a simple quantum mechanical picture we provide a probability analysis that rationalizes the ~10% population of species in the TS region during the first few ps as indicated by the experiment.

The black curve in Fig. 1A shows the initial ($t<0$ ps) unpumped XAS O K-edge spectrum of atomic O and CO co-adsorbed on Ru(0001) (*17, 19*). The resonance at 530.8 eV is the signature

of the adsorbed O atom as an O 2*p*-Ru 4*d* antibonding state, here denoted O 2*p**, that resides just above the Fermi level (*20*). The spectral feature at 533.8 eV is the 2π* resonance of adsorbed CO (*16, 21*) and the broad structure at 542 eV is related to adsorbed O as an O 2*p*-Ru 5*sp* shape resonance (*22*).

With a delay of ~1 ps after excitation by a 400-nm laser pulse, the XAS spectrum changed dramatically, as shown in red in Fig. 1A. We observed four distinct major spectral changes with respect to the unpumped spectrum. These changes were visualized in more detail after curve-fitting the pumped spectrum with four new spectral components together with 90% of the unpumped spectrum; to account for the increased translational, non-reactive motion, the position of the CO 2π* level was let free and shifted to lower energy, similar to the case of pure CO on Ru(0001) after 400 nm laser excitation (*15*). We observed a low-energy component at 529.8 eV in the O related O 2*p** feature indicating activation of the O atoms. Additional intensity appeared between the O 2*p** and CO 2π* resonances at 532 eV that was neither present upon laser excitation of CO adsorbed separately on Ru(0001) (*15*), nor seen in spectrum calculations of O displacement toward lower coordination in the coadsorbate system. We saw a shoulder on the high-energy side of the 2π* resonance distinguished more clearly in the curve fitting as a broad resonance at 535.6 eV and there was additional intensity appearing at higher energies that could be approximated as a broad feature centered at 539 eV. The intensity in this region was fitted with two separate Gaussians in order to incorporate the features predicted from our spectrum calculations.

Figure 1B shows the transient changes of these spectral features in terms of delay from the laser pump (*19*). In spite of the shot-by-shot statistical uncertainties in the x-ray spectra with spurious effects already before the optical pulse, significant and systematic changes are evident in Fig. 1B. The O 2*p** intensity shows a rapid increase on a 280±100 fs timescale (*19*) which can be regarded as almost instantaneous within our time-resolution. This time-scale is similar to the thermalization time of femtosecond laser excited electrons in Ru (*23*) such that both thermalized and non-thermalized electrons may contribute (*8*,*11*). The shift in the CO 2π* occurs on a timescale of 550±120 fs and the new state between the O 2*p** and CO 2π* appears on the same 800±250 fs timescale as the additional intensity in the region 536-539 eV (*19*).

In order to shed more light on the molecular species that give rise to these additional spectral features we turn to density functional theory calculations of XAS spectra (*19, 24*) based on structures found along the minimum energy reaction path. Figure 2A shows the calculated pathway from the initial state (IS), where the CO is adsorbed at an on-top site and O in a hollow site, to the highest TS (TS1), where O and CO have come into chemical contact with the O atom in the bridge site and CO in a near-hollow site with a small 16° tilt from the surface normal. Beyond TS1, we find a rather flat descending region that ends with an abrupt change in energy giving a small barrier (TS2), which corresponds to a bent, weakly chemisorbed CO_2 species that has a 34° tilt and where, along the CO—O reaction coordinate, there is still a bond elongation in comparison to the expected final state (FS) with CO_2 released into gas phase with substantial kinetic energy (*25*). To analyze the reaction further we compute the potential of mean force (*16*), including contributions from entropy, as a function of the reaction coordinate. Figure 2A shows that TS1 and TS2 become stabilized relative to the IS at higher temperatures but otherwise there are no dramatic changes.

Figures 2B and C show the calculated O K-edge spectra of O and CO along the reaction path. In Fig. 2C we observe a red-shifted O 2*p** peak for O in a near-bridge-position which we relate to the intensity at 529.8 eV in the experiment. Focusing on the changes between IS and TS1, Fig. 2B shows a shift of 1 eV in the CO 2π* position towards lower energy, into the region between the O and CO resonances where we observed an increase in intensity in the experimental data. Such a shift has been established previously for CO on Ni(100) where co-adsorbed hydrogen generates a mixed on-top and hollow phase where the experimental XAS spectrum shows a shift of 2 eV between the two adsorption sites (*26*). This result is similar to the O 1*s* binding energy shift observed with x-ray photoelectron spectroscopy (*27*). The computed shift is consistent with the present experimental data but seems to be underestimated. The CO 2π* shift is similar for TS2. We denote this spectral component O*C—O since it is the O atom in the CO molecule that mostly contributes the spectral intensity.

In TS1 a weak OC—O bond is formed with an elongated bond distance of 1.7 Å compared to 1.2 Å in the CO_2 molecule. The sigma bond within a molecule gives rise to an anti-bonding shape resonance whose energy position is sensitive to the bond length (*28*). In Fig. 2C we note that the computed OC—O* shape resonance, mostly located on the O atom, is at 535.5 eV which nicely corresponds to the intensity appearing on the high-energy side of the CO 2π* resonance after the laser-pump. Figure 2C shows that this resonance shifts to higher energy at 540 eV in the TS2 state because of a shorter OC—O bond length. There is not much contribution in the pumped experimental data at 540 eV indicating less population of TS2 but, as discussed above, there is substantial intensity around 538-539 eV indicating species with bond lengths between TS1 and TS2. Figure 2D shows a nearly linear dependence between bond length and resonance position in the computed OC—O shape resonance energy position until the bond length becomes similar to the other internal C-O bond and the two resonances delocalize (*28*), as seen in CO_2. Because the pumped spectra from Fig. 1 can be fit with two broad OC—O resonances, there are species of various bond lengths contributing to the experimental data. This corresponds to population of several points around TS1 and on the path toward TS2 as the activated species undergo several attempts to react, where the majority does not pass over the barrier, however, but dissociate back to O and CO.

Let us now address the transient populations as a function of delay time between the optical and x-ray laser pulses. Within the time resolution of the experiment, Fig. 1B shows an almost instantaneous O 1*s* shift to lower energy consistent with O moving from the hollow site toward the bridge site (Fig. 2C). The activation of CO is somewhat slower, where the 500 fs transient is within the time resolution of previous measurements of pure CO on Ru(0001) (*15*). These studies concluded that excitation of frustrated rotations (*29*) leads to translational motion on the surface (*15*).

Femtosecond laser-induced reactions are typically explained in terms of photoexcitation of substrate electrons leading to thermalized electrons at a high temperature and subsequent heating of the substrate phonons (Fig. 3A), which on ruthenium takes place on a time-scale of approximately 1-2 picoseconds (*13*). The reaction is thus driven via energy transfer from the electron or phonon systems to the adsorbates. The observed sub-picosecond timescale is consistent with a dominating excitation process involving electrons in the substrate (*13, 15, 30*),

with weaker coupling for the CO molecule than for O, leading to a slower response. The spectral changes associated with TS1 and the region between TS1 and TS2 in terms of the O*C—O and OC—O* resonances both have the same transient of 800 fs suggesting population of the same class of configurations. These spectral components reach a maximum in intensity after around 1 ps as shown in Fig. 1B. Since most of the energy to reach the transition state is related to the activation of the oxygen atom we followed the contrast at the low energy side of the spectra that decays on a timescale of a few ps (*19*). This indicates vibrationally excited atomic motions as in a thermal process making the species undergo several attempts to react. The two broad overlapping components between 535 and 541 eV in the fit of the experimental spectrum indicate that there is a distribution of transient species of various OC—O bond lengths. This is further corroborated by the rather constant intensity of all observed transient species between 1 and 3 ps.

In the fit of the experimental data in Fig. 1A there is roughly a 10 % population of species in the TS region between 1.5 and 3 ps. Figure 3 demonstrates that this is consistent with a sufficiently highly excited vibrational state. Figure 3B shows the vibrational wave function probability distribution for different quantum states in the CO and O potential well up to TS1 from Fig. 2A. Highly excited vibrational states clearly have large amplitude at the turning points where, in a classical picture, the motion slows down. We estimate the probability (*19*) of finding O and CO in the CO_2 TS region as indicated in Fig. 3B based on an elevated adsorbate temperature obtained from ultrafast energy transfer from transiently excited substrate electrons (*19*). With an estimated peak adsorbate temperature of 1500-3300 K (Fig. 3A) we find a transient population of the TS region up to ~10 % (Fig. 3C). The majority of these species are reflected back to O and CO at the barrier but still have a significant probability of populating the vicinity of the classical turning point in the TS region. We note that CO_2 molecules formed from reactants passing over the barrier are expected to desorb with excess translational energy from a hot state rather than forming an intermediate chemisorbed state (*25*). The origin of the low transmission coefficient over the barrier to the CO_2 final product is an open question where friction leading to non-adiabatic processes could play an important role and will require further theoretical work.

From the above observations we summarize the findings based on a simple picture as depicted in Fig. 4. The O becomes activated with motions parallel to the surface on a timescale below 300 fs whereas CO is activated on a 500 fs timescale. They will start to collide on the surface since the CO is caged by O atoms in neighboring sites in the coadsorbed honeycomb structure (*19*). These collisions generate a transient population of species around the TS region that appears on timescales slightly longer than the initial motion of the CO and O species. Most collisions lead to dissociation back to CO and O with subsequent further collisions into TS and only a small fraction of the events result in the formation of CO_2 as seen in the low reaction yield (11).

We thus experimentally observe species near and beyond the rate-determining barrier at TS1, *i.e.* also in the rather flat region between TS1 and TS2 as shown in Fig. 2A. Although unexpected, this is not surprising given that both classically and quantum mechanically, transit over a potential energy barrier entails a deceleration as kinetic energy is converted to potential energy. The ability to probe transient species close to the TS opens completely new insights into the electronic states of reacting molecules at surfaces and it provides theory with an unprecedented benchmark in the description of surface-catalyzed processes. We anticipate that this will provide

an essential tool to underpin our fundamental understanding of surface chemical processes in heterogeneous catalysis.

References:

1. J. C. Polanyi, A. H. Zewail, *Acc. Chem. Res.* **28**, 119-132 (1995).
2. A. Stolow, A. E. Bragg, D. M. Naumark, *Chem. Rev.* **104**, 1719-1757 (2004).
3. P. I. Ionov, S. I. Ionov, C. Wittig, *J. Chem. Phys.* **107**, 9457-9463 (1997).
4. A. J. Orr-Erwing, *J. Chem. Phys.* **140**, 090901 (2014).
5. N. F. Scherer, C. Sipes, R. B. Bernstein, A. H. Zewail, *J. Chem. Phys.* **92**, 5239-5259 (1990).
6. G. Ertl, *Reactions at Solid Surfaces*. (John Wiley&Sons, 2009).
7. J. K. Nørskov, F. Studt, F. Abild-Pedersen, T. Bligaard, *Fundamental Concepts in Heterogeneous Catalysis*. (Wiley, 2014).
8. H. Petek, *J. Chem. Phys.* **137**, 091704 (2012).
9. J. A. Prybyla, T. F. Heinz, J. A. Misewich, M. M. T. Loy, J. H. Glownia, *Phys. Rev. Lett.* **64**, 1537 (1990).
10. F.-J. Kao, D. G. Busch, D. Cohen, D. Gomes da Costa, W. Ho, *Phys. Rev. Lett.* **71**, 2094 (1993).
11. T.-H. Her, R. J. Finlay, C. Wu, E. Mazur, *J. Chem. Phys.* **108**, 8595 (1998).
12. M. Bonn, S. Funk, C. Hess, D. Denzler, C. Stampfl, M. Scheffler, M. Wolf, G. Ertl, *Science* **285**, 1042-1045 (1999).
13. C. Frischkorn, M. Wolf, *Chem. Rev.* **106**, 4207 (2006).
14. P. Szymanski, A. L. Harris, N. Camillone III, *J. Phys. Chem. C* **112**, 15802-15808 (2008).
15. M. Beye, T. Anniyev, R. Coffee, M. Dell'Angela, A. Föhlisch, J. Gladh, T. Katayama, S. Kaya, O. Krupin, A. Møgelhøj, A. Nilsson, D. Nordlund, J. K. Nørskov, H. Öberg, H. Ogasawara, L. G. M. Pettersson, W. F. Schlotter, J. A. Sellberg, F. Sorgenfrei, J. Turner, M. Wolf, W. Wurth, H. Öström, *Phys. Rev. Lett.* **110**, 186101 (2013).
16. M. Dell'Angela, T. Anniyev, M. Beye, R. Coffee, A. Föhlisch, J. Gladh, T. Katayama, S. Kaya, O. Krupin, J. LaRue, A. Møgelhøj, D. Nordlund, J. K. Nørskov, H. Öberg, H. Ogasawara, H. Öström, L. G. M. Pettersson, W. F. Schlotter, J. A. Sellberg, F. Sorgenfrei, J. Turner, M. Wolf, W. Wurth, A. Nilsson, *Science* **339**, 1302-1305 (2013).
17. T. Katayama, T. Anniyev, M. Beye, R. Coffee, M. Dell'Angela, A. Föhlisch, J. Gladh, S. Kaya, O. Krupin, A. Nilsson, D. Nordlund, W. F. Schlotter, J. A. Sellberg, F. Sorgenfrei, J. Turner, M. Wolf, W. Wurth, H. Öström, H. Ogasawara, Ultrafast soft x-ray emission spectroscopy of surface adsorbates using a x-ray free electron laser. *J. El. Spec. Rel. Phen.* **187**, 9 (2013)
18. W. F. Schlotter, J. J. Turner, M. Rowen, P. Heimann, M. Holmes, O. Krupin, M. Messerschmidt, S. Moeller, J. Krzywinski, R. Soufli, M. Fernandez-Perea, N. Kelez, S. Lee, R. Coffee, G. Hays, M. Beye, N. Gerken, F. Sorgenfrei, S. Hau-Riege, L. Juha, J. Chalupsky, V. Hajkova, A. P. Mancuso, A. Singer, O. Yefanov, I. A. Vartanyants, G. Cadenazzi, B. Abbey, K. A. Nugent, H. Sinn, J. Luning, S. Schaffert, S. Eisebitt, W. S. Lee, A. Scherz, A. R. Nilsson, W. Wurth, *Rev. Sci. Instrum.* **83**, 7724 (2012).
19. Details of the materials and methods, and supporting analysis of the experimental and theoretical data, are available at *Science* Online.
20. A. Nilsson, L. G. M. Pettersson, B. Hammer, T. Bligaard, C. H. Christensen, J. K. Nørskov, *Catal. Lett.* **100**, 111-114 (2005).

21. C. Keller, M. Stichler, G. Comelli, F. Esch, S. Lizzit, D. Menzel, W. Wurth, *Phys. Rev. B* **57**, 11951 (1998).
22. E. O. F. Zdansky, A. Nilsson, H. Tillborg, O. Björneholm, N. Mårtensson, J. N. Andersen, R. Nyholm, *Phys. Rev. B* **48**, 2632 (1993).
23. M. Lisowski, P. A. Loukakos, U. Bovensiepen, J. Stähler, C. Gahl, M. Wolf, *Appl. Phys. A* **78**, 165-176 (2004).
24. L. Triguero, L. G. M. Pettersson, H. Ågren, *Phys. Rev. B* **58**, 8097 (1998).
25. C. Hess, S. Funk, M. Bonn, D. N. Denzler, M. Wolf, G. Ertl, *Appl. Phys. A* **71**, 477-483 (2000).
26. H. Tillborg, A. Nilsson, N. Mårtensson, J. N. Andersen, *Phys. Rev. B* **47**, 1699 (1993).
27. H. Tillborg, A. Nilsson, N. Mårtensson, *Surf. Sci.* **273**, 47 (1992).
28. J. Stöhr, *NEXAFS Spectroscopy*. G. Ertl, R. Gomer, D. L. Mills, Eds., Springer Series in Surface Science (Springer-Verlag, Berlin-Heidelberg, 1992).
29. M. Bonn, C. Hess, S. Funk, J. Miners, B. N. J. Persson, M. Wolf, G. Ertl, *Phys. Rev. Lett.* **84**, 4653-4656 (2000).
30. A. C. Luntz, in *Chemical Bonding at Surfaces and Interfaces,* A. Nilsson, L. G. M. Pettersson, J. K. Nørskov, Eds. (Elsevier, 2008).

Acknowledgments:
This work is supported by the US Department of Energy, Basic Energy Science through the SUNCAT Center for Interface Science and Catalysis, the Swedish National Research Council, the Knut and Alice Wallenberg foundation, the US Department of Energy through the SLAC Laboratory Directed Research and Development program under contract DE-AC02-76SF00515, the Volkswagen Stiftung and the DFG within the excellence cluster "Center for Ultrafast Imaging (CUI)". The spectrum calculations were performed on resources provided by the Swedish National Infrastructure for Computing (SNIC) at the HPC2N center. Portions of this research were carried out on the SXR Instrument at the Linac Coherent Light Source (LCLS), a division of SLAC National Accelerator Laboratory and an Office of Science user facility operated by Stanford University for the U.S. Department of Energy. The SXR Instrument is funded by a consortium whose membership includes the LCLS, Stanford University through the Stanford Institute for Materials Energy Sciences (SIMES), Lawrence Berkeley National Laboratory (LBNL), University of Hamburg through the BMBF priority program FSP 301, and the Center for Free Electron Laser Science (CFEL). The experimental and theoretical data are available in the SM.

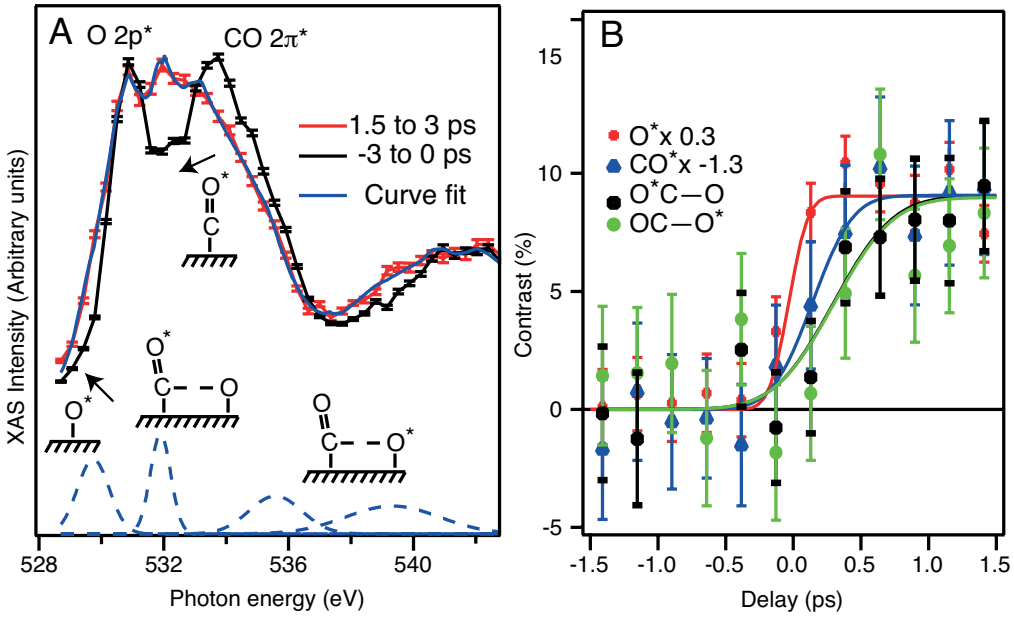

Figure 1. (A) Pump-probe O K-edge XA spectrum of CO/O/Ru(0001). The black line and markers show as reference the spectrum averaged over the 3 ps right before the arrival of the pump pulse and the red line and markers, the spectrum averaged over the interval between 1.5 and 3 ps after the arrival of the laser pump. Averaging is performed to reduce noise. The solid blue line shows a curve fit obtained from a weighted sum of the unpumped XA spectrum and the four Gaussians plotted with dashed blue lines in the bottom of the figure, with a red-shift of the CO 2π* due to external vibrational motion taken into account. The inset cartoons schematically depict the microscopic interpretation of the laser-induced spectral changes and the arrows indicate the direction of spectral shifts as the O and CO species move out from their equilibrium sites. (B) Time-development of the spectral intensities in four different spectral regions plotted as the contrast (difference between the pumped and un-pumped experimental data normalized to the sum of the intensities and scaled to have the same asymptotes (*19*)); The red dots (O*) show the contrast on the low-energy side of the O 2*p** that corresponds to activation of adsorbed O. Note the very fast (280 fs) change in contrast following the pump laser. The blue triangles (CO*) show the contrast on the CO 2π* resonance where a negative contrast appears on a 550 fs time-scale (reversed in the figure for easy comparison of slopes (*19*)), corresponding to a loss of intensity after laser irradiation due to activation of external vibrations in the adsorbed CO. The black squares (O*C—O) and green circles (OC—O*) show the contrast around the O-CO π* and O-CO σ*, respectively. Both show a transient increase in the contrast on a time-scale of 800 fs. The Poisson error bars are shown.

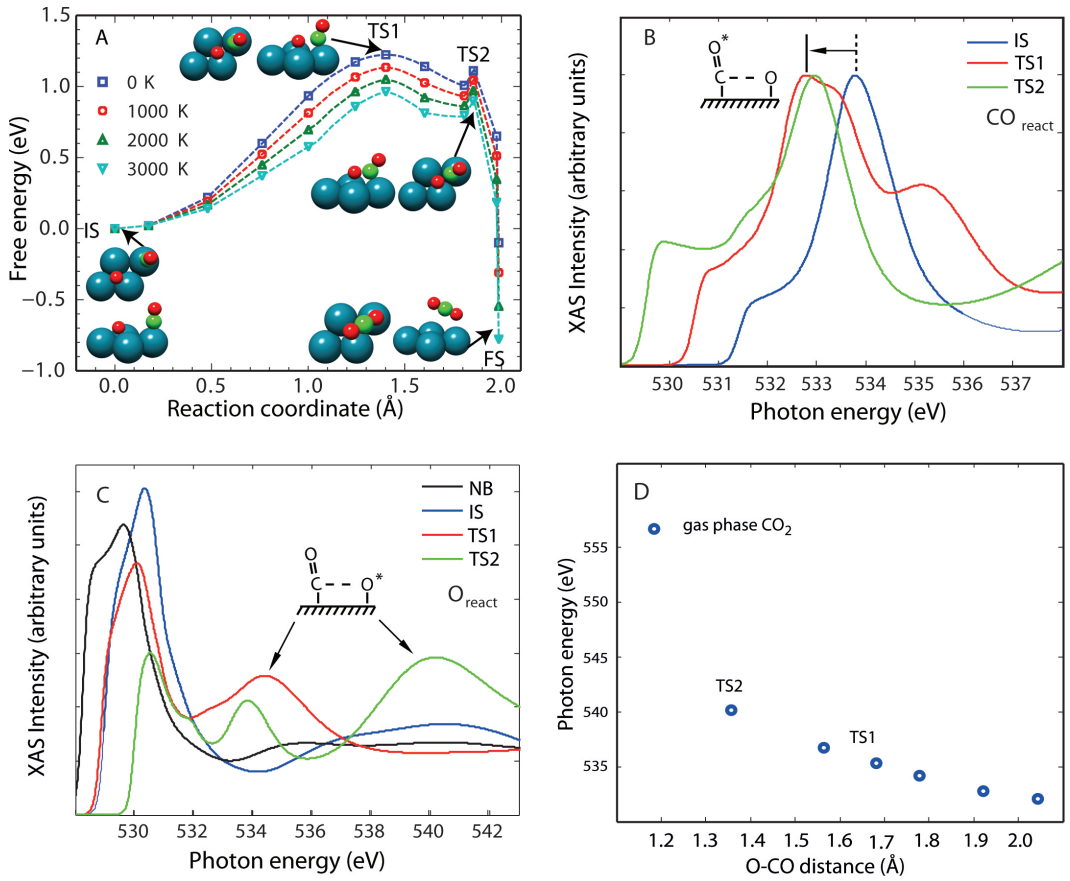

Figure 2. (A) The free energy for CO oxidation on Ru(0001) at 0 K (minimum energy path), 1000 K, 2000 K, and 3000 K. In order to put the initial state (IS) structure at the origin, the reaction coordinate is defined as $d_{\text{O-CO}}$(IS) - $d_{\text{O-CO}}$(X), where $d_{\text{O-CO}}$ is the distance between the reacting O atom and the C atom in the adsorbed CO molecule, and X is the position along the reaction path, from the IS to the final state (FS). The surface structures (top and side view) of the IS, TS1, TS2 and FS are shown. (B and C) Computed XAS O K-edge spectra of selected geometries projected on the reacting CO (B) or O (C). In (C) the XAS spectrum for a separate configuration denoted NB (near-bridge) in which atomic O is situated close to a bridge site in the co-adsorbate system is also shown. (D) The computed energy of the shape resonance (see Fig. 2C, where it is mainly located on the O atom at ~540 eV in TS2) arising from OC—O bond formation is plotted against the OC—O bond length for a number of different geometries along the reaction path. The linear trend is broken as the resonance position of gas phase CO_2 is included at ~557 eV.

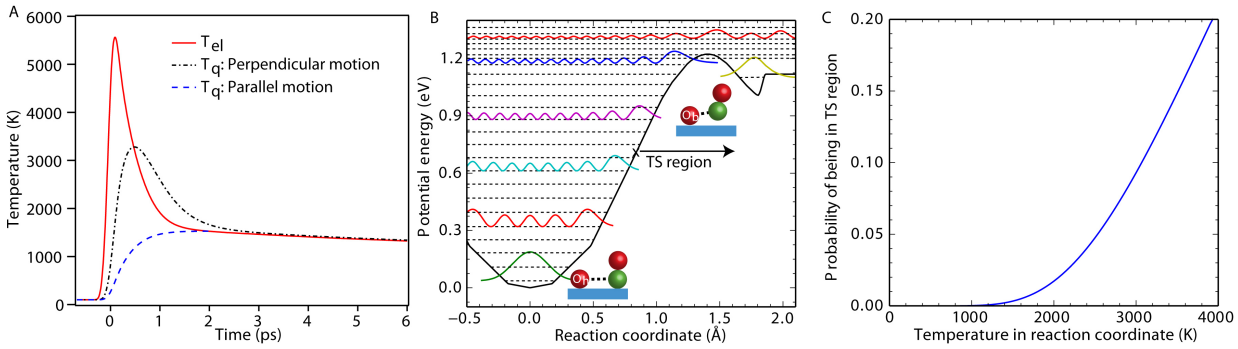

Figure 3. Time-evolution of the temperature and probability analysis for forming O-CO near-TS complexes on Ru(0001). (A) Based on the two-temperature model and *ab initio* electronic friction of O atoms on Ru(0001) (*19*), the peak values of the adsorbate temperature in the relevant O-Ru vibrational modes are estimated to be 1500-3300 K in the time-range between 0.5 and 3 ps after the laser excitation. (B) Minimum energy path for CO oxidation where the left side, approaching a different O atom, is not shown for simplicity (*19*). Dashed lines are energy eigenvalues and solid lines represent the corresponding probability density distribution at selected energy levels. The TS region is defined from the inflection point (arrow) of the minimum energy path out to 2 Å. (C) Probability of finding O-CO complexes within the TS region as a function of the adsorbate temperature in the reaction coordinate. The peak values of the adsorbate temperature lead to a potential population of the TS region of up to ~10 %.

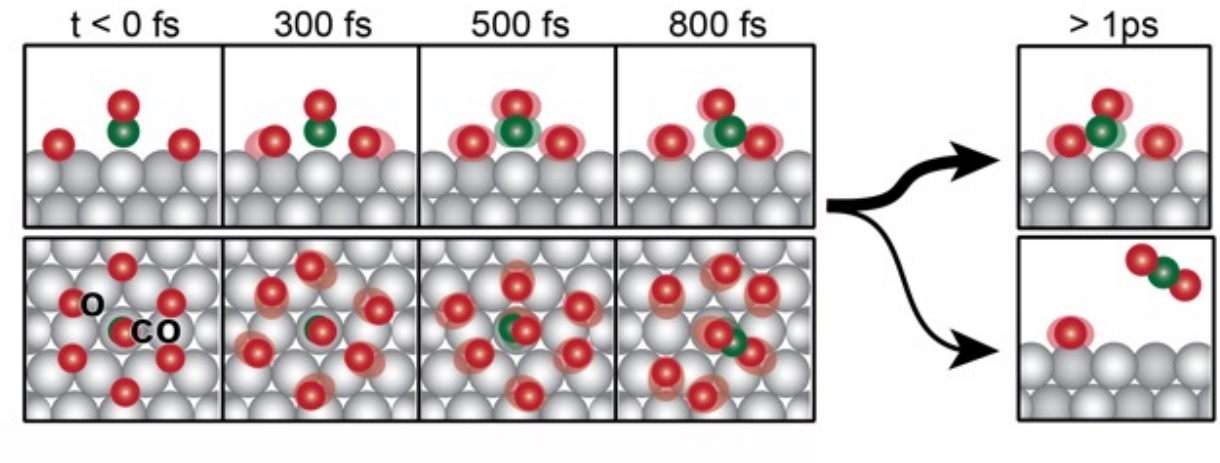

Figure 4. Pictorial side and top views of the reaction sequence with the corresponding time scales for oxygen activation, CO translation, collisions that lead to form the transition state and either dissociation back to reactants and further collisions into the transition state or, with lower probability, to the final CO_2 reaction product.